PHYSICAL REVIEW B **79**, 161401(R) (2009)

# Growth of oxide-metal interfaces by atomic oxygen: Monolayer of NiO(001) on Ag(001)

A. Rota,[1] S. Altieri,[1] and S. Valeri[1,2]
[1]*CNR-INFM National Center on Nanostructures and Biosystems at Surfaces (S3), via G. Campi 213/a, 41100 Modena, Italy*
[2]*Dipartimento di Fisica, Universitá di Modena e Reggio Emilia, via G. Campi 213/A, 41100 Modena, Italy*
(Received 19 February 2009; published 1 April 2009)

We have tested the use of atomic oxygen to prepare 3*d* oxide-metal interfaces for which standard reactive deposition techniques based on molecular oxygen fail in providing well-defined chemical composition and controlled atomic structure and morphology. Using monolayer NiO(001) on Ag(001) as a model system, we find that NiO(001)/Ag(001) films grown by atomic oxygen have a two-dimensional highly stoichiometric $(1\times1)$ structure and a uniform monoatomic thickness, while those grown by conventional $O_2$ have a nonstoichiometric $(2\times1)$ structure or a three-dimensional morphology. Atomic oxygen may provide a practical way to prepare 3*d* oxide-metal interfaces with highly controlled stoichiometry, structure, and morphology.

DOI: 10.1103/PhysRevB.79.161401 PACS number(s): 68.47.Gh, 68.55.−a, 68.37.Ef, 79.60.−i

A central issue of modern materials physics and nanoscience is the control at atomic scale of chemical and structural interface abruptness in complex heterostructures through atomic-layer control of the growth processes.[1] Having ultimate control over the thickness and structure of one to three monolayer (ML) oxide film on a metal substrate may allow tuning electronic structure and properties of heterogeneous catalysts.[2,3] More generally, nanometric oxide films on metals may have unprecedented properties determined by the ultrathin thickness as well as the presence of the oxide-metal interface.[2–5]

The use of molecular oxygen ($O_2$) during ultrahigh-vacuum (UHV) deposition of a metal element, the so-called reactive deposition, is the standard way to grow stoichiometric and epitaxial alkaline-earth and 3*d* metal oxide films with thickness larger than a few monolayers on various metallic substrates.[4–9] This method is also useful to prepare a chemically and structurally well-defined single atomic layer of strongly ionic wide band gap oxide such as MgO(001) on Ag(001).[4,8] Nevertheless, standard $O_2$-based reactive deposition fails in the case of more covalent 3*d* oxide-metal interfaces, as shown by pioneering works[10–14] of Sebastian *et al.*,[10,11] Hagendorf *et al.*,[12,14] Shantyr *et al.*,[13] and Wollschläger *et al.*[15] on ML NiO and CoO on Ag(001) and on Pt(111) recently confirmed by Caffio *et al.*,[16,17] Giovanardi *et al.*,[18] and, for monolayer NiO on Pd(001), by Agnoli *et al.*[19,20] Monolayer NiO exhibit nonstoichiometric two-domain $(2\times1)$ structure and $c(4\times2)$ defective structure on Ag(001) (Refs. 10 and 15–18) and on Pd(001),[19,20] respectively, while even more complicated different phases coexist for monolayer amount of Ni-O deposited on Pt(111).[14] Similarly, monolayer amounts of CoO deposited on Ag(001) yield the simultaneous formation of monoatomic CoO(001) and CoO(111), and biatomic CoO(111) islands with complex growth morphology.[11–13]

Attempts to circumvent this complex growth behavior adopting different combinations of substrate temperature, $O_2$ partial pressure, and deposition rate, as well as postannealing treatment either in $O_2$ atmosphere or in UHV, turned out to be inefficient since the properties of NiO and CoO monolayer deposited by $O_2$ on Ag(001), on Pd(001), and on Pt(111) drastically depend on the growth parameters,[10–20] with strong changes in the chemical nature, atomic structure, and overall morphology, even for minor variations in $O_2$ pressure and deposition/annealing temperature. For sufficiently high growth and/or annealing temperature, a well-oxidized NiO and CoO single phase can be obtained on Ag(001), which however aggregates in multilayer islands with a minimum thickness of two atomic planes.[10–14,16,17] The chemical composition of NiO monolayer on Ag(001) was partly improved by drastically increasing the $O_2$ growth pressure up to $Ni/O_2$ ratio of about 1/1000, but the interface morphology in this case remained unknown.[18]

In another work, Chambers and Droubay[21] grew chromium and iron oxide ultrathin films on Pt(111) by oxygen plasma assisted deposition and showed that epitaxial $\alpha$-$Cr_2O_3$ and $\alpha$-$Fe_2O_3$ films can be grown on Pt(111) as a chemically and structurally well-defined single $(1\times1)$ phase only for thickness larger than 5 ML, while under the same oxidizing conditions well-oxidized and nonreconstructed epitaxial $\alpha$-$Cr_2O_3$ and $\alpha$-$Fe_2O_3$ films can be grown on insulating oxide substrates also at smaller thickness down to 1 ML.[22] Similarly, well-stoichiometric and atomically nonreconstructed $(1\times1)$ epitaxial single monolayer NiO and CoO films can be grown on oxide substrates[23,24] but not on metal substrates.[10–20]

Despite the intense research in the field, the important question of why structurally and chemically well-defined 3*d* oxide monolayer films can be easily grown on insulating substrates but not so on metallic substrate to date has not yet been addressed in the literature. This is exactly the issue that we address in this work. Here we suggest that the peculiar growth properties of 3*d* oxide-metal interfaces may be a result of the competition between two main opposite processes involving 3*d* adatoms on a metal surface exposed to an oxidizing gas, namely, an oxidation process due the gas molecules and a reduction process due to electron transfer and/or hybridization from the underneath metal surface. Our basic idea is that under extreme oxidizing conditions it could be possible to make the oxidation much more efficient than the reduction process, with the consequent formation of a well-defined ionic crystal phase which is stabilized by Madelung potentials and image potential interactions at the oxide-metal interface,[5] thus preventing the formation of a reconstructed and off-stoichiometric oxide layer.

To test this idea we have used a beam of pure atomic oxygen to grow 1 ML NiO(001)/Ag(001) film that we have analyzed *in situ* by x-ray photoelectron spectroscopy (XPS),

 

low energy electron diffraction (LEED), and scanning tunneling microscopy (STM). Atomic oxygen is one of the most aggressive available oxidizing agents. Moreover, monolayer NiO(001) on Ag(001) is well suited to check our model since, among the 3*d* transition metals, nickel is the species with the highest reluctance toward oxidation when supported on an electron donor reservoir such as a metal substrate, as shown by the ratio $R=E_A/E_I$ between the electron affinity and the 3*d* ionization potential that, within our model, provides a quantitative measure of the difficulty to oxidize 3*d* atoms on metal surfaces (for Sc, Ti, V, Cr, Fe, Co, Ni, and Cu *R* values are 0.2, 0.1, 0.7, 0.4, 0.2, 0.6, 2.3, and 0.5, respectively). We find that monolayer NiO(001)/Ag(001) films grown by atomic oxygen have a two-dimensional highly stoichiometric $(1\times1)$ structure and a uniform monoatomic thickness, in contrast with those grown by conventional $O_2$.

The experiments were performed in a UHV ($P_{base}<5\times10^{-11}$ Torr) setup hosting an epitaxial oxide film growth chamber connected to Omicron variable temperature (VT) STM, multichannel XPS/Auger, and LEED analysis facilities.[25] NiO(001) films were epitaxially grown at a rate of about 0.2 ML/min on a well-ordered Ag(001) single crystal kept at 470 K by evaporating high-purity Ni from a Knudsen effusion cell and simultaneously dosing atomic oxygen obtained by flowing $O_2$ through a Oxford TC-50 thermal cracker operated at a cracking efficiency >50%, with a total oxygen background pressure of $3\times10^{-7}$ Torr. We have verified that at this $O_2$ pressure molecular oxygen is not able to oxidize the Ni deposited on silver so that the formation of the NiO oxide film on Ag(001) under our experimental conditions is entirely due to atomic oxygen. Quartz microbalance and high-resolution transmission electron microscopy (HRTEM) experiments on 10 ML NiO(001)/Ag(001) showed that the grown films have a nice layered structure with sharp NiO/Ag interfaces and provided a direct calibration of the total absolute amount of deposited NiO which was then compared with the NiO fractional coverage measured by STM in the range of 0.2–1.0 ML. In separate experiments we have directly dosed Ag(001) with atomic oxygen in the absence of Ni adatoms and verified through STM, XPS, and LEED that, under the chosen growth conditions, the silver surface remains chemically, structurally, and morphologically inert toward atomic oxygen over a time scale at least three times larger than the 1 ML NiO(001)/Ag(001) deposition time. For each given NiO (sub)monolayer coverage, several samples were prepared and analyzed at 300 K following alternated STM, XPS/Auger, and LEED analytical sequences. STM images were recorded in constant current mode using chemically etched W and Pt-Ir tips at different positive bias voltages. Integral XPS spectral intensities were analyzed after standard x-ray satellite filtering and Shirley background subtraction.

Figures 1(a) and 1(b) displays Al $K_\alpha$ excited O 1*s* and Ni 2*p* XPS spectra of 0.3, 0.6, and 1 ML NiO(001)/Ag(001) films, together with Ni 2*p* of bulk Ni metal and cleaved NiO single crystal measured under the same conditions. The O 1*s* spectra have a single peak at 529.0 eV [Fig. 1(a)] with no signs of high binding energy satellites characteristic of hydroxyl groups and nonstoichiometric oxides.[25] The Ni 2*p* of the monolayer films closely resemble the published spectra

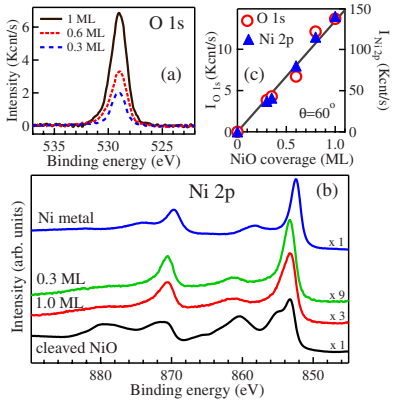


FIG. 1. (Color online) (a) O 1*s* and (b) Ni 2*p* XPS of 0.3, 0.6, and 1 ML NiO(001)/Ag(001) films, bulk Ni metal, and cleaved NiO; (c) O 1*s* and Ni 2*p* intensities at increasing NiO coverage.

of well-oxidized $Ni^{2+}$ ions on Ag(001),[18] with a large chemical shift of 1 eV to high binding energy compared to Ni metal [Fig. 1(b)]. In particular, the Ni 2*p* threshold to satellite splitting, which is a well-known fingerprint of the photoemitting atom chemical state and the related multiplet structure,[26] in the monolayer spectra (7.9 eV) is similar to that of cleaved NiO (7.2 eV) rather than to that of Ni metal (5.9 eV). Moreover, apart from a modest spectral broadening with increasing coverage, no Ni 2*p* line shape changes are observed going from 0.3 to 1 ML [Fig. 1(b)]. In contrast, a sudden line shape change occurs above 1 ML so that the Ni 2*p* of the 3 ML film is very similar to that of cleaved NiO [Fig. 2(a)]; consistent with the fact that the electronic structure of 1 ML NiO(001)/Ag(001) is well distinguishable from that of 3 ML and thicker NiO(001)/Ag(001) films.[27]

As shown in Fig. 1(c), the integrated intensity of both O 1*s* and Ni 2*p* spectra increases at a constant rate with NiO deposition, thus indicating that the ratio between nickel and oxygen atoms remains constant during the film growth. In order to check whether this Ni/O ratio corresponds to that of stoichiometric NiO, we have measured the intensity ratio $(I_{Ni\,2p}/I_{O\,KLL})$ of Ni 2*p* and O $KL_{23}L_{23}$ spectra recorded within the same spectroscopic experiment from films and cleaved NiO [Fig. 2(a)]. For 0.3, 0.6, 1, and 3 ML NiO(001)/

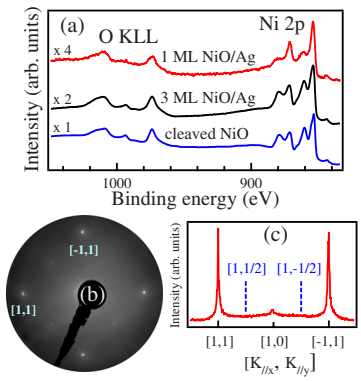


FIG. 2. (Color online) (a) Ni 2*p* XPS and O *KLL* Auger spectra of 1 and 3 ML NiO(001)/Ag(001), and cleaved NiO; (b) LEED pattern of 1 ML NiO(001)/Ag(001) at $E_p=94$ eV; (c) intensity profile across the [1,1] and [−1,1] spots in (b) showing the absence of fractional order spots.

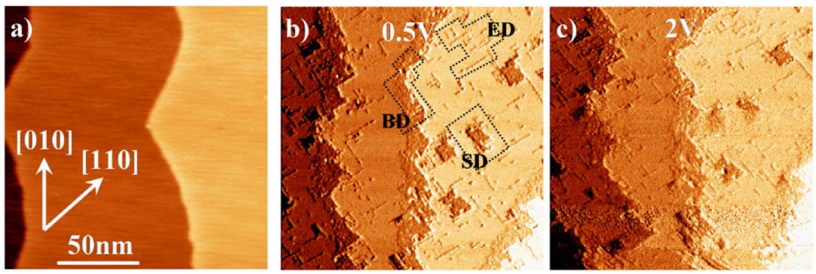


FIG. 3. (Color online) STM topographic image of (a) clean Ag(001) recorded at 0.5 V, and 0.3 ML NiO(001)/Ag(001) at (b) 0.5 and (c) 2 V.

Ag(001), we find $I_{\mathrm{Ni}\,2p}/I_{\mathrm{O}\,KLL}$ values which differ from that obtained on stoichiometric cleaved NiO single crystal by less than 7%. To check the correctness of this method for determining the stoichiometric composition of our NiO films, we have verified that the value of $I_{\mathrm{Ni}\,2p}/I_{\mathrm{O}\,KLL}$ measured on a cleaved NiO and on NiO(001)/Ag(001) films does not depend on the XPS take-off angle, implying that Ni $2p$ and O $KL_{23}L_{23}$ electrons have comparable escape depth, as indeed expected since they have similar kinetic energies. A further confirmation of the good stoichiometric composition and well-ordered atomic structure of our monolayer films is provided by the LEED pattern of 1 ML NiO(001)/Ag(001) measured at $E_p$=94 eV and displayed in Fig. 2(b). The pattern has a square $(1\times1)$ symmetry with no signs [Fig. 2(c)] of the $(2\times1)$ superstructure due to nonoxidized metallic nickel reported for $O_2$ reactive deposition of Ni on Ag(001).[10,15–18] LEED patterns similar to that in Fig. 2(b) were systematically observed for 0.3, 0.6, and 0.85 ML NiO(001)/Ag(001) films.

Figure 3(a) displays a typical topographic image of the clean Ag(001) substrate showing three wide and flat monoatomic silver terraces with regular edges $0.20\pm0.01$ nm high. The deposition of 0.3 ML NiO strongly modifies the surface morphology as shown in Fig. 3(b) reporting an STM image recorded at 0.5 V bias. Extended squarelike structures (SD) $5\times15$ to $15\times30$ nm$^2$ wide and narrow elongated (ED) structures 5–30 nm long and 0.6–1.2 nm wide are visible on flat silver terraces after film deposition. Both types of structures appear as depressions with rather sharp edges oriented parallel to the ⟨110⟩ crystal directions [Fig. 3(b)]. Moreover, the silver step edges look strongly reoriented along ⟨110⟩ directions, and the morphology of the terrace regions extending up to 15–20 nm from the silver kinks and running along the entire step edges appears substantially modified upon NiO film deposition [BD in Fig. 3(b)]. The measured topographic depth of both the SD and the BD depressions is $0.28\pm0.05$ nm, while that of the narrow ED is $0.15\pm0.05$ nm. The different depth value found for the ED might be related to limited resolution tip effects showing up more effectively while imaging narrow structures. In any case, these measured topographic depths are strongly different from the characteristic interplanar spacing in both silver and nickel oxide. This finding is similar to earlier STM reports by Sebastian *et al.*[10,11] who showed that submonolayer deposition of NiO on Ag(001) appears in topographic images at low bias as depressions, with depth strongly different from Ag and bulk NiO lattice spacing. Moreover, apart from a general image worsening due to high voltage instability intrinsic to STM experiments on oxide covered metal surfaces, the SD, ED, and BD depressions did not show any voltage-dependent contrast [Figs. 3(b) and 3(c)]. This is yet another typical behavior reported for monoatomic NiO islands on Ag(100), which has been used to distinguish between monoatomic and multilayered oxide islands on metals surfaces since the latter exhibits STM topographic height that strongly changes with bias in the range of 0.5 and 2 V.[10–13,28] Finally, we would like to remark that the measured topographic depth of the ED, SD, and BD features indicates that these depressions observed in Figs. 3(b) and 3(c) cannot be due to empty Ag surface vacancies since in our STM experiments monoatomic Ag steps correctly have a topographic height of 0.20 nm so that Ag surface vacancies on flat silver terraces would indeed appear as 0.20-nm-deep depressions.

Based on the above arguments, we assign SD, ED, and BD structures to monoatomic NiO islands on Ag(001). Support to this interpretation is also provided by recent theoretical work by Ferrari *et al.*[29,30] showing that monoatomic oxide islands on flat silver terraces have a tendency to grow embedded within the metal surface, with edges oriented along the ⟨110⟩ directions. This prediction matches the experimental STM observation by Sebastian *et al.*[10,11] on submonolayer NiO on Ag(001) and is consistent with the ⟨110⟩ edge orientation of ED and SD structures observed in Fig. 3(b). In order to verify whether the ED, SD, and BD structures in Fig. 3(b) are indeed due to deposited NiO islands with monoatomic height, we have measured their statistical recurrence averaged over different surface positions for several freshly prepared samples. We found a fractional coverage corresponding to $0.24\pm0.04$ ML, which closely matches the independently known value of 0.3 ML in total absolute amount of deposited NiO calibrated by HRTEM and quartz microbalance. This is exactly what is expected for NiO islands growing on Ag(001) with a uniform monoatomic thickness. An additional support to this conclusion is provided by the absence of voltage-dependent STM surface topography changes showing the absence of bi- and multilayered NiO/Ag islands [Figs. 3(b) and 3(c)].[10,11]

In Fig. 4(a) we display a topographic image of 0.85 ML NiO(001)/Ag(001) recorded at 0.5 V. The image shows a wide central terrace (A) containing a squared island (B) about $20\times20$ nm$^2$, plus three narrower terraces (C, D, and E). The edges of the squared B island are parallel to the ⟨110⟩ crystal directions, while the step edges of the elongated terraces look more irregular. The difference in topographic height between A-B, A-C, C-D, and D-E terraces is 0.21 nm, i.e., equal to the Ag(001) interplanar spacing. This indicates that A, B, C, D, and E are monoatomic silver terraces uniformly covered by NiO deposit.[10,11] Voltage-dependent topo-

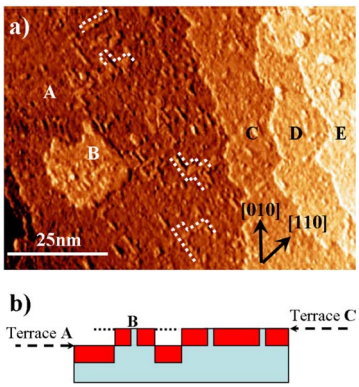


FIG. 4. (Color online) STM topographic image of (a) 0.85 ML NiO(001)/Ag(001) at 0.5 V; (b) side-view sketch of (a).

graphic images revealed that for 0.85 ML NiO(001)/Ag(001) deposition the fraction of double layer NiO islands is limited to below some percent of a monolayer. Apart from this, we did not detect any substantial voltage-dependent topography changes, thus supporting the conclusion that the deposited 0.85 ML NiO/Ag(001) film has a highly uniform monoatomic thickness.[10,11]

To further confirm the atomic thickness of the deposited NiO layer, we have analyzed in more detail the surface morphology displayed in Fig. 4(a). At closer inspection, two different types of structures are visible on the surface of terraces A, B, C, D, and E, namely, narrow structures of about $1\times10$ nm$^2$ and polygonal structures of about $10\times10$ nm$^2$, both with a topographic height of approximately 0.15 nm and edges well aligned parallel to the $\langle 110\rangle$ directions. These features in Fig. 4(a) recall the ED and SD structures observed in Figs. 3(b) and 3(c) but with a substantial difference: while the features in Fig. 3(b) systematically appear as *depressions*, those in Fig. 4(a) always appear as *protrusions*. This suggests that while the ED and SD features in Fig. 3(b) are due to deposited NiO, as discussed above, those in Fig. 4(a) are instead due to silver regions not covered by NiO. This assignment is consistent with earlier STM work by Sebastian *et al.*[10] reporting that submonolayer NiO(001)/Ag(001) islands appear in STM images always surrounded by protruding Ag ridges. We have thus measured the statistical recurrence of the narrow elongated and the polygonal structures in Fig. 4(a), finding a fractional coverage corresponding to $0.14\pm0.05$ ML, which closely matches the expected fraction of uncovered silver surface for a deposition of 0.85 ML NiO film grown on Ag as a single monoatomic layer. Once again, this is indeed what is expected for NiO islands growing on Ag(001) with a highly uniform monoatomic thickness.

In summary, we have been able to show that atomic oxygen allows control at the atomic scale of chemical and structural interface abruptness and provides ultimate control over the thickness and morphology of NiO(001)/Ag(001) oxide-metal interfaces, not achievable by conventional $O_2$ reactive deposition. Based on our growth model and on the observation that within the 3*d* series Ni atoms exhibit the highest reluctance toward oxidation when placed on a metal surface, we expect that similar results can be obtained for other 3*d* oxide-metal interfaces. Our results point to a practical way toward preparing 3*d* oxide-metal interfaces with highly controlled stoichiometry, structure, and morphology, thus enlarging the materials basis to grow systems with potentially unprecedented chemical-physical properties determined by their subnanometer thickness.

S.A. acknowledges financial support by CNR-INFM-S3 National Center through project *Seed Activity* and thanks S. A. Chambers for useful discussions.

[1] N. Nakagawa *et al.*, Nature Mater. **5**, 204 (2006).
[2] M. Sterrer, T. Risse, U. M. Pozzoni, L. Giordano, M. Heyde, H. P. Rust, G. Pacchioni, and H. J. Freund, Phys. Rev. Lett. **98**, 096107 (2007).
[3] G. Pacchioni, L. Giordano, and M. Baistrocchi, Phys. Rev. Lett. **94**, 226104 (2005).
[4] S. Altieri, L. H. Tjeng, F. C. Voogt, T. Hibma, and G. A. Sawatzky, Phys. Rev. B **59**, R2517 (1999).
[5] S. Altieri, L. H. Tjeng, F. C. Voogt, T. Hibma, O. Rogojanu, and G. A. Sawatzky, Phys. Rev. B **66**, 155432 (2002).
[6] S. A. Chambers, Surf. Sci. Rep. **39**, 105 (2000).
[7] M. C. Gallagher *et al.*, Surf. Sci. Lett. **339**, L909 (1995).
[8] S. Schintke, S. Messerli, M. Pivetta, F. Patthey, L. Libioulle, M. Stengel, A. De Vita, and W. D. Schneider, Phys. Rev. Lett. **87**, 276801 (2001).
[9] C. Lamberti, E. Groppo, C. Prestipino, S. Casassa, A. M. Ferrari, C. Pisani, C. Giovanardi, P. Luches, S. Valeri, and F. Boscherini, Phys. Rev. Lett. **91**, 046101 (2003).
[10] I. Sebastian *et al.*, Faraday Discuss. **114**, 129 (1999).
[11] I. Sebastian *et al.*, Surf. Sci. **454-456**, 771 (2000).
[12] C. Hagendorf *et al.*, Surf. Sci. **532-535**, 346 (2003).
[13] R. Shantyr *et al.*, Thin Solid Films **464-465**, 65 (2004).
[14] C. Hagendorf *et al.*, Phys. Chem. Chem. Phys. **8**, 1575 (2006).
[15] J. Wollschläger *et al.*, Thin Solid Films **400**, 1 (2001).
[16] M. Caffio *et al.*, J. Phys. Chem. B **108**, 9919 (2004).
[17] M. Caffio *et al.*, J. Phys.: Condens. Matter **18**, 2379 (2006).
[18] C. Giovanardi, A. di Bona, and S. Valeri, Phys. Rev. B **69**, 075418 (2004).
[19] S. Agnoli *et al.*, Surf. Sci. **576**, 1 (2005).
[20] S. Agnoli *et al.*, J. Phys. Chem. B **109**, 17197 (2005).
[21] S. A. Chambers and T. Droubay, Phys. Rev. B **64**, 075410 (2001).
[22] S. A. Chambers, Y. Liang, and Y. Gao, Phys. Rev. B **61**, 13223 (2000).
[23] D. Alders, F. C. Voogt, T. Hibma, and G. A. Sawatzky, Phys. Rev. B **54**, 7716 (1996).
[24] S. D. Peacor *et al.*, Surf. Sci. **301**, 11 (1994).
[25] S. Altieri, S. F. Contri, and S. Valeri, Phys. Rev. B **76**, 205413 (2007).
[26] A. E. Bocquet, T. Mizokawa, T. Saitoh, H. Namatame, and A. Fujimori, Phys. Rev. B **46**, 3771 (1992).
[27] F. Cinquini, L. Giordano, G. Pacchioni, A. M. Ferrari, C. Pisani, and C. Roetti, Phys. Rev. B **74**, 165403 (2006).
[28] S. Valeri, S. Altieri, U. del Pennino, A. di Bona, P. Luches, and A. Rota, Phys. Rev. B **65**, 245410 (2002).
[29] A. Ferrari, S. Casassa, and C. Pisani, Phys. Rev. B **71**, 155404 (2005).
[30] A. M. Ferrari *et al.*, Surf. Sci. **588**, 160 (2005).